Bulletin of Mathematical Biology (2024) 86:34
https://doi.org/10.1007/s11538-024-01259-3

Society for Mathematical Biology

ORIGINAL ARTICLE

First Passage Times of Long Transient Dynamics in Ecology

Grant R. Poulsen[1] · Claire E. Plunkett[1] · Jody R. Reimer[1,2]

Received: 28 October 2023 / Accepted: 10 January 2024

Abstract
Long transient dynamics in ecological models are characterized by extended periods in one state or regime before an eventual, and often abrupt, transition. One mechanism leading to long transient dynamics is the presence of ghost attractors, states where system dynamics slow down and the system lingers before eventually transitioning to the true attractor. This transition results solely from system dynamics rather than external factors. This paper investigates the dynamics of a classical herbivore-grazer model with the potential for ghost attractors or alternative stable states. We propose an intuitive threshold for first passage time analysis applicable to both bistable and ghost attractor regimes. By formulating the first passage time problem as a backward Kolmogorov equation, we examine how the mean first passage time changes as parameters are varied from the ghost attractor regime to the bistable one, through a saddle-node bifurcation. Our results reveal that the mean and variance of first passage times vary smoothly across the bifurcation threshold, eliminating the deterministic distinction between ghost attractors and bistable regimes. This work suggests that first passage time analysis can be an informative way to classify the length of a long transient. A better understanding of the duration of long transients may contribute to greater ecological understanding and more effective environmental management.

Keywords First passage time · Ghost attractor · Long transients · Regime shift · Saddle-node bifurcation

1 Introduction

Recent work has highlighted the existence and importance of long transient dynamics in ecological models (Hastings 2001; Hastings et al. 2018; Boettiger and Batt 2020; Morozov et al. 2020). Long transient dynamics refer to model trajectories that linger

✉ Jody R. Reimer
jody.reimer@utah.edu

1 Department of Mathematics, University of Utah, Salt Lake City, UT, USA

2 School Of Biological Sciences, University of Utah, Salt Lake City, UT, USA

Published online: 23 February 2024

near a state or attractor for a long time (e.g., many generations) before transitioning—often rapidly— to a different attractor (Hastings et al. 2018). Such sustained but ultimately transient dynamics can arise through several mechanisms, and can occur in both deterministic and stochastic models (Hastings et al. 2021; Morozov et al. 2020). Recently, the mathematical theory of long transients, including formal definitions and exploration of conditions necessary for their existence, has started to take shape (Liu and Magpantay 2022; Liu et al. 2023; Morozov et al. 2020).

Long transient dynamics are interesting not only mathematically, but also for their ecological implications. If a population, community, or ecosystem is experiencing long transient dynamics, this can make management or conservation of the system challenging. A population at equilibrium may be managed very differently than one that is in a long transient period (Boettiger 2021), and mistaking long transient dynamics for a steady state, or vice versa, may result in lost resources and ecological disasters (Francis et al. 2021).

One mechanism by which long transient dynamics arise is through a so-called ghost attractor (Strogatz 1994; Hastings et al. 2018). This is a state near which system dynamics are very slow, causing the system to spend considerable time near the ghost attractor before eventually rapidly transitioning to the true attractor. Ghost attractors have been studied in theoretical models (Vortkamp et al. 2020) as well as empirical studies (Jäger et al. 2008; Van Geest et al. 2007). The dynamics caused by a ghost attractor may appear qualitatively similar to those caused by tipping points or regime shifts (Boettiger and Batt 2020; Carpenter et al. 2011; Dakos et al. 2019). However, the rapid transition between the long transient dynamics and the asymptotic dynamics is driven solely by dynamics inherent to the system rather than a change in parameter values or an external forcing of the state variable.

One way in which a ghost attractor occurs is if the system has a saddle-node bifurcation and parameter values are just next to the bifurcation point, adjacent to where the two steady states collide and disappear. Dynamics near this collision state— the ghost of the attractor that disappeared in the bifurcation— will be very slow, causing the system to linger in its vicinity. In noisy systems, it can be difficult to infer whether a system has a ghost attractor or a true attractor (Reimer et al. 2021; Abbott and Nolting 2017). In a system with two stable states, stochasticity can cause a population to jump from one basin of attraction to another, so that both a bistable regime and a regime with a ghost attractor generate similar bimodal distributions of states over time (Abbott and Dakos 2021; Abbott and Nolting 2017).

One property of interest in this scenario is the timing of the jump from one state to another, either from a ghost attractor to the true attractor, or between two alternate stable states. Using simulation, Reimer et al. (2021) found that adding noise to a model with a ghost attractor alters the mean trajectory (Figure 2 in Reimer et al. (2021)), but that work did not explore what effects the timing of the jump and how it varies as the parameters are shifted across the saddle-node bifurcation.

For stochastic models with alternative stable states, several approaches exist for understanding stochasticity-induced jumps between basins of attractions, including Kramers escape probabilities (Kramers 1940; Zhang et al. 2019) and first passage time (FPT) analysis (Abbott and Dakos 2021; Chou and D'Orsogna 2014; Grebenkov et al. 2020). The FPT of a dynamical system is the earliest time $t_\beta > 0$ at which a

state variable x reaches a chosen threshold β. For deterministic models, the FPT is a deterministic quantity. For stochastic models, however, the FPT is a random variable that can be described by a probability density function. We can then examine properties of this probability density function such as the mean FPT (MFPT). Depending on the nature of the stochasticity, the MFPT can be estimated using Monte Carlo simulations of the system (Abbott and Dakos 2021; Drury 2007), approximated using various approximation methods (Drury 2007; Kurella et al. 2015; Nolting and Abbott 2016), or found by means of the backward Kolmogorov equation (Floris 2019; Gardiner et al. 1985; McKenzie et al. 2009).

In a bistable model, the threshold used for a MFPT analysis is, intuitively, often the value of the unstable equilibrium that separates them. In a model with a ghost attractor, however, this natural choice of threshold no longer exists, and yet the concept of how long the system spends near the ghost attractor seems like it should lend itself to a MFPT anlaysis, provided a suitable threshold can be found for when the long transient period is finished.

In this paper, we work with the classical herbivore-grazer model of May (1977), which is capable of either a ghost attractor or alternative stable states, depending on parameter regime. We propose an intuitive threshold for a FPT analysis that can be used in both a bistable and ghost attractor regimes. We formulate the FPT problem as a backward Kolmogorov equation, which we solve to examine how the MFPT of the system changes as parameters are varied through a saddle-node bifurcation. We find that the MFPT and the variance of FPTs vary smoothly as we cross the bifurcation threshold, eliminating the distinction between the ghost attractor and bistable regimes seen in a purely deterministic model.

2 Herbivore-Grazer Model

We first introduce the deterministic harvest-grazer model of May (1977). This model has been used to explore early-warning signs of critical transitions (Scheffer et al. 2009), how noise can induce transitions between high and low vegetation states (alternate stable states) (Zhang et al. 2019), and for its potential to produce long transient dynamics (Reimer et al. 2021).

This model describes a plant population of size x with logistic population growth and subject to grazing,

$$\frac{dx}{dt} = rx\left(1 - \frac{x}{K}\right) - \frac{ax^q}{x^q + h^q}. \tag{1}$$

Grazing is represented using a Holling Type III functional response, with half-saturation constant h, maximum grazing rate a, and shape parameter q. Two saddle-node bifurcations are possible for this model under certain parameterizations (May 1977). If we vary a, the number of non-zero steady states jumps from one, to three, and then back to one as a passes two bifurcation thresholds (a_1 and a_2 in Fig. 1). For parameter values between these two bifurcation thresholds, this model has two alternative stable states; a smaller herbivore-dominated state and a larger vegetation-

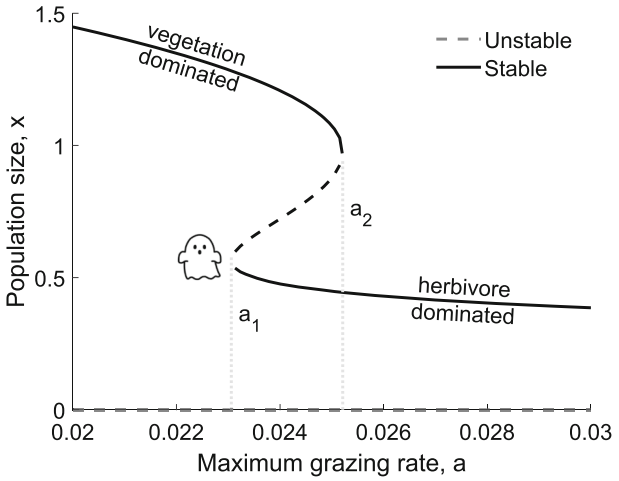

Fig. 1 Bifurcation structure of the deterministic herbivore-grazer model (1) as the maximum grazing rate, a, is varied. Two saddle-node bifurcations occur at $a_1 \approx 0.0232$ and $a_2 \approx 0.0252$. Other parameters are $r = 0.05$, $K = 2$, $h = 0.38$, and $q = 5$

dominated state (Ludwig et al. 1978). A ghost attractor occurs for values of a adjacent to the bifurcation points (i.e., slightly less than a_1 and slightly greater than a_2). For these values of a, (1) approaches, but does not achieve, a value of 0, for values of x near the ghost attractor, causing the population size to change very slowly in this region and appear nearly stable (Fig. 2). The closer a is to the bifurcation value, the longer the population may spend near the ghost attractor. However, because it is not a true attractor, the population eventually leaves the ghost attractor, followed by a rapid approach to the true steady state.

To study the effects of environmental stochasticity on these dynamics, we consider the related Itô stochastic differential equation,

$$\begin{aligned} dX &= \left[rX\left(1 - \frac{X}{K}\right) - \frac{aX^q}{X^q + h^q} \right] dt + \sigma X dW \\ &= \mu(X)dt + \phi(X)dW \end{aligned} \tag{2}$$

where W is stationary Gaussian white noise, scaled by the product of the population size X and a noise constant σ. This is a Wiener process with drift vector $\mu(X)$ and diffusion vector $\phi(X)$.

Following (Reimer et al. 2021), we fix parameters as follows: $r = 0.05$, $K = 2$, $h = 0.38$, and $q = 5$, and vary a around the bifurcation value $a_1 \approx 0.023$. We consider solutions with the initial values $x(0) = 0.3$ and $X(0) = 0.3$. Note that while we focus on a_1 here, a similar analysis could be completed for a_2.

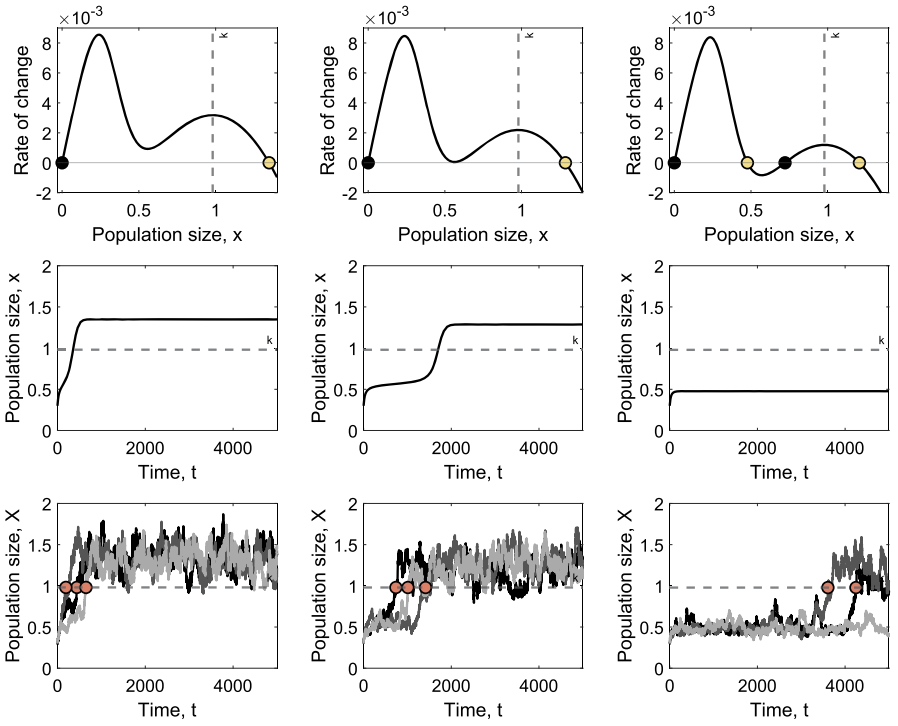

Fig. 2 Illustration of how the deterministic model (1) and stochastic model (2) behavior varies with a, the maximum grazing rate. As we move from the left column to the right, the system transitions from having a single nonzero steady state ($a = 0.022$), to having a ghost attractor ($a = 0.023$), and then across a saddle-node bifurcation resulting in a bistable system ($a = 0.0245$). The top row shows the rate of population change (right hand side of [1)], with black and yellow circles marking unstable and stable steady states. The middle row shows the corresponding deterministic trajectories. The bottom row shows three solutions to the stochastic model (2), with their FPTs highlighted as pink circles. The FPT threshold is shown in each plot as a dashed black line. In the final plot, one of the trajectories did not exceed the threshold in the shown time period, so its FPT is not marked. Observe the clear differences in behavior in the deterministic trajectories, compared with the blurrier distinction between the different stochastic plots. Parameters are $r = 0.05$, $K = 2$, $h = 0.38$, $q = 5$, $\phi = 0.02$, and $x_0 = 0.3$. The thresholds for $a = 0.022$, 0.023, and 0.024 are $\beta = 0.9807$, 0.9798, and 0.9787 respectively (Color figure online)

3 First Passage Time Analysis

3.1 Defining the Threshold

We need to define a threshold β for our FPT analysis that intuitively corresponds to the population transition from the lower state of interest (either the true attractor or the ghost attractor, depending on parameterization regime) to the higher, vegetation-dominated steady state. To achieve this, we chose β as the value of x that maximizes dx/dt over the interval between either the ghost attractor or the unstable steady state and the larger vegetation-dominated stable steady state (dashed lines in Fig. 2). This corresponds to the state at which the population is transitioning most rapidly towards

the vegetation-dominated stable steady state in the deterministic model. These values were calculated numerically as the largest root of the derivative of (1) with respect to x, and were found to vary nonlinearly with a (Appendix Fig. 5).

3.2 Formulation as a Backwards Kolmogorov Equation

We can now solve the FPT problem using the backward Kolmogorov equation (Allen 2010; Floris 2019). We first define a reliability function, $r(t; x_0)$, as the probability that a given time t is less than the FPT t_β of a stochastic process, for a given initial condition x_0 (Floris 2019),

$$r(t; x_0) = P(t < t_\beta | x_0). \tag{3}$$

The complement of this function, $1 - r(t; x_0)$, is the probability that the first passage has occurred by time t. Its time derivative, which we will denote as $q(t; x_0)$, provides us with a probability density function for the FPT,

$$q(t; x_0) = \frac{\partial}{\partial t}\left[1 - r(t; x_0)\right] = -\frac{\partial}{\partial t} r(t; x_0). \tag{4}$$

We now work obtain an expression for the reliability function, since we can then use it to derive the probability distribution of FPTs.

Let $p(x, t; x_0)$ denote the transition probability density function of (2), which provides the relative likelihood of the population transitioning from the initial condition $X(0) = x_0$ to state x at time t. Since (2) is time-homogeneous, $p(x, t; x_0)$ is a solution of the backward Kolmogorov equation

$$\frac{\partial p(x, t; x_0)}{\partial t} = \mu(x_0) \frac{\partial p(x, t; x_0)}{\partial x_0} + \frac{1}{2}\phi^2(x_0) \frac{\partial^2 p(x, t; x_0)}{\partial x_0^2}. \tag{5}$$

For $x_0 \in (\alpha, \beta)$, where $\alpha \geq 0$ and β is our threshold value, we can obtain the reliability function $r(t; x_0)$ by integrating the transitional probability density function,

$$r(t; x_0) = \int_0^\beta p(x, t; x_0) dx. \tag{6}$$

By integrating both sides of (5) from 0 to β with respect to x, we see that $r(t; x_0)$ also satisfies the backward Kolmogorov equation,

$$\frac{\partial r(t; x_0)}{\partial t} = \mu(x_0) \frac{\partial r(t; x_0)}{\partial x_0} + \frac{1}{2}\phi^2(x_0) \frac{\partial^2 r(t; x_0)}{\partial x_0^2} \tag{7}$$

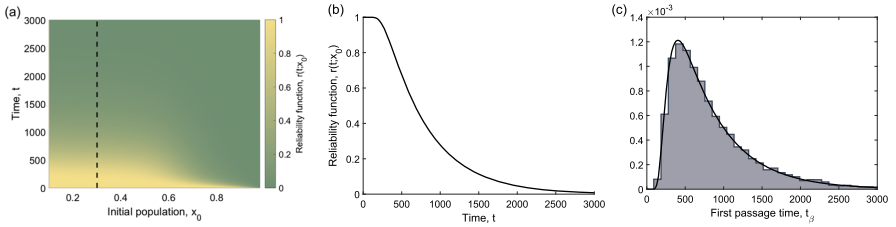

Fig. 3 **a** Reliability function, $r(t; x_0)$, obtained as the numerical solution to the backward Kolmogorov Equation (7). The black dashed line indicates the solution for $x_0 = 0.3$, which is plotted in (**b**). **c** The probability density function of FPTs, $q(t; x_0)$, obtained as the negative time-derivative of the curve in (**b**). The histogram shows the frequency of FPTs in 10,000 stochastic solutions, confirming the probability density curve. The solution shown corresponds to the ghost attractor regime, where $a = 0.023$. Other parameters are $r = 0.05$, $K = 2$, $h = 0.38$, $q = 5$, and $\phi = 0.02$

To obtain the reliability function, we solve (7) with the following initial and boundary conditions:

$$\begin{aligned} \text{initial condition}: \quad & r(x_0, 0) = 1 \\ \text{boundary conditions}: \quad & r(\beta, t) = 0, \quad r(\alpha, t) = 1. \end{aligned} \tag{8}$$

We numerically solve (7)–(8) to obtain $r(t; x_0)$ (Fig. 3a, b). We then take its time derivative to find the probability density function of FPTs $q(t; x_0)$, following (4). Comparing this solution to the empirical probability density function obtained through 10,000 Monte Carlo solutions of (2), supports the calculations (Fig. 3c).

4 Moments of the Distribution of First Passage Times

Once we have obtained the probability density function of FPTs, $q(t; x_0)$, we can explore how it changes as we vary a through the bifurcation value a_1 by looking at its moments. The MFPT of the stochastic model varies smoothly as a increases through the ghost attractor regime and through the bifurcation point a_1 (Fig. 4a). For comparison, we also calculated the FPT of the deterministic model (1), which displays a vertical asympote at $a = a_1$, since the solution will never leave the basin of attraction that contains x_0 (Fig. 4). The difference between the FPT of the deterministic model and the MFPT of the stochastic model is greatest in the region of the ghost attractor, very near the bifurcation value of a.

We also looked at how the variance of the FPT probability density function varies with a. For values of $a > a_1$, the variance increases dramatically (Fig. 4b, c).

5 Sensitivity to Noise Intensity

Until this point, we have held all parameters except a to be constant. Here we briefly also explore the effect of varying σ, the noise intensity parameter in (2), on our findings. As we increase and decrease σ (we looked at values in the range of $[0.015, 0.025]$,

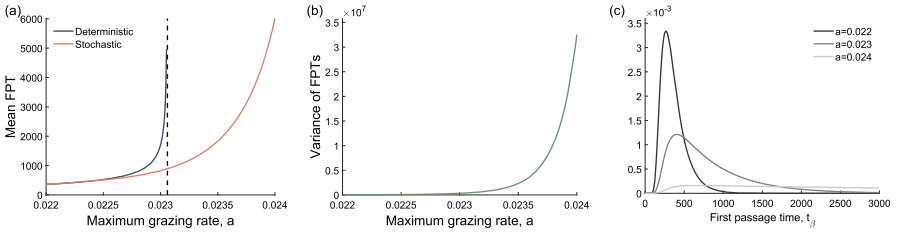

Fig. 4 **a** Mean FPTs of the stochastic herbivore-grazer model (2) as the maximum grazing rate, a, is varied through the bifurcation value a_1 (dashed vertical line). The FPT of the corresponding deterministic model (1) is shown for comparison. **b** Variance of FPTs. **c** Probability density functions of FPTs for three representative value of a, corresponding to regimes with a single stable steady state, a ghost attractor, and a bi-stable regime, illustrating the shift in the mean and increase in variance as a increases. Parameters are $r = 0.05$, $K = 2$, $h = 0.38$, $q = 5$, $\phi = 0.02$, and $x_0 = 0.3$

higher and lower than the value of $\sigma = 0.02$ used previously), we find that the MFPT does not vary monotonically with σ, but rather its behavior depends on the value of a (Appendix Fig. 6). If a is small (vegetation dominated regime), then the MFPT increases with σ. For the bistable regime with a larger a, the MFPT instead decreases with σ. Finally, for intermediate values (near the ghost attractor), the MFPT is nonmonotonic in σ. The variance of FPTs also depends on σ and a; for $a < a_1$, the variance of FPTs increases with σ, while for $a > a_1$, it decreases (Appendix Fig. 7.) However, the qualitative patterns of dependence of the MFPT on a observed in Fig. 4 still hold for all values of σ considered.

6 Discussion

In this paper, we used the classic herbivore-grazer model by May (1977) to explore how the FPT of a stochastic trajectory changes as model parameters are varied through ghost attractor into a bistable regime. We introduced an intuitive threshold for FPT analysis, applicable to both the bistable and ghost attractor scenarios. We were able to obtain the full distribution of FPTs by formulating the problem as a backward Kolmogorov equation. Solving the this equation allowed us to investigate how the MFPT and variance of FPTS evolve as parameters are varied through a saddle-node bifurcation. Our findings indicate that both the MFPT and the variance of FPTs exhibit smooth changes as we traverse the bifurcation threshold. This effectively erases the distinction between the ghost attractor and bistable scenarios observed in a purely deterministic model. For all parametrizations considered, the MFPT of the stochastic model was less than the FPT of the deterministic model. This difference between the FPT of the deterministic versus stochastic model was found to be greatest as we approached the bifurcation point, where the system displays a ghost attractor.

These findings align with those of Abbott and Nolting (2017), who found that stochastic time series in a unistable regime can masquerade as those in a bistable regime. Under certain conditions, stochastic time series generated by Abbott and Nolting (2017) from both regimes had similar mean and equilibrium population sizes, temporal variance in population sizes, and had similar results from various statistical

tests for bimodality. We here suggest that the distribution of FPTs provides another metric with which to evaluate the distinction between regimes.

Previous work by Reimer et al. (2021) examined the same grazer-herbivore model in an effort to determine which statistical methods may allow for inference regarding whether a time series resulted from the ghost attractor or bistable regimes. By averaging over multiple simulated trajectories, they found that the average trajectory diverges from the ghost attractor earlier than the corresponding deterministic trajectory, i.e., $FPT(\mathrm{E}[X]) < FPT(x)$. While related, this is different than what we consider in this paper: $\mathrm{E}[FPT(x]$. For example, when $a = 0.023$, $FPT(\mathrm{E}[X]) = 842$ and $\mathrm{E}[FPT(x)] = 831$. This discrepancy is due to Jensen's inequality and the nonlinearity of the MFPT. Since typically only one stochastic trajectory may be realized in a system, rather than a simultaneous ensemble of trajectories, the full distribution of possible FPTs, as considered in this paper, likely provides more relevant information for understanding possible outcomes.

Recently proposed more formal definitions of what constitutes long transient behavior have been based on the idea that the length of the transient can be made arbitrarily long if some controlling parameter p is chosen appropriately (Liu et al. 2023; Morozov et al. 2020). Morozov et al. (2020) outline two possible ways by which this can happen, either (i) there exists a finite critical parameter value p_c such that the length of the transient approaches infinity as $p \to p_c$, or (ii) the length of the transient approaches infinity as $p \to \infty$. For the deterministic herbivore-grazer model explored here, we find ourselves in case (i), where the FPT$\to \infty$ as $a \to a_1^-$. However, the addition of multiplicative noise to create the stochastic model instead results in case (ii), where the MFPT$\to \infty$ as $a \to \infty$ (Fig. 4a). Whether this is a universal or even common result of adding multiplicative noise to a deterministic model with a long transient remains an open question.

The approach taken here, of finding the full distribution of FPTs using the backward Kolmogorov approach, can be applied to a variety of models with long transient dynamics, provided they can be formulated as a stochastic differential equation. This approach allows for characterisation of the expected duration of a long transient as well as the variance of this duration. However, depending on the mechanism behind the long transient (e.g., crawl-by behavior, slow-fast dynamics, attractor hopping, etc. [Morozov et al. 2020)], the challenge will lie in defining a suitable threshold for FPT analysis.

Code Availability Computations were conducted using R (version 4.3.1; R Core Team (2023)) and MATLAB (version 9.9.0.1570001, R2020b; The MathWorks Inc. (2020)). All code and full documentation are archived at doi:10.5281/zenodo.10472441.

Appendix

A Supplementary figures

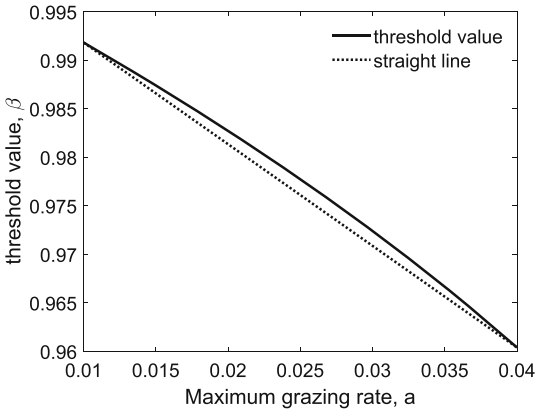

Fig. 5 Illustration of the nonlinearity of the thresholds, β, chosen for our FPT analysis as we vary a. A straight line (dashed) is plotted for comparison. Note that the two saddle-node bifurcations occur at $a_1 \approx 0.0232$ and $a_2 \approx 0.0252$. Other parameters are $r = 0.05$, $K = 2$, $h = 0.38$, and $q = 5$

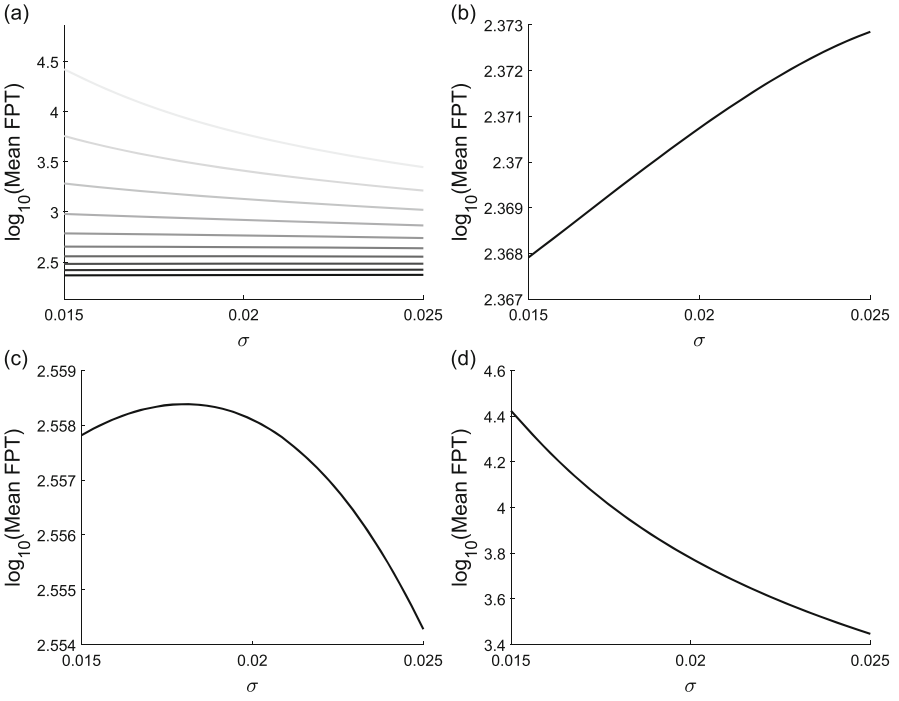

Fig. 6 Exploration of how the MFPT changes with the noise constant σ. **a** How the MFPT varies as σ is varied depends on the value of a. Curves correspond to 10 evenly spaced values of a between 0.0210 (bottom, darkest curve) and 0.0240 (top, lightest curve). The y axis uses a log10 scaling for ease of visualization. **b–c** A closer look at three of the curves in (**a**), illustrating that the MFPT may increase, decrease, or be non-monotonic as σ is varied, depending on the value of a. Values of a in (**b–c**) are $a = 0.021$, 0.022, and 0.024, respectively. Other parameters are $r = 0.05$, $K = 2$, $h = 0.38$, and $q = 5$

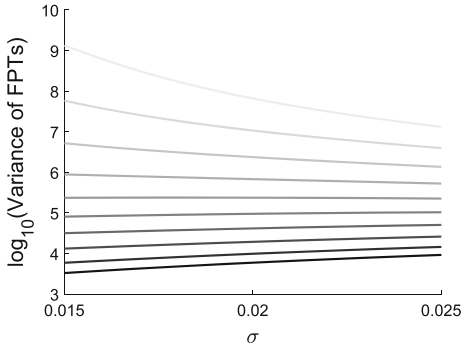

Fig. 7 Exploration of how the variance of FPTs changes as the noise constant σ is varied around the value used elsewhere in the paper ($\sigma = 0.02$). As in Fig. 6, the y axis uses a log10 scaling for ease of visualization and curves correspond to 10 evenly spaced values of a between 0.0210 (bottom, darkest curve) and 0.0240 (top, lightest curve). Other parameters are $r = 0.05$, $K = 2$, $h = 0.38$, and $q = 5$

References

Abbott KC, Dakos V (2021) Mapping the distinct origins of bimodality in a classic model with alternative stable states. Thyroid Res 14:673–684

Abbott KC, Nolting BC (2017) Alternative (un) stable states in a stochastic predator-prey model. Ecol Complex 32:181–195

Allen LJ (2010) An introduction to stochastic processes with applications to biology. CRC Press, Boca Raton

Boettiger C (2021) Ecological management of stochastic systems with long transients. Thyroid Res 14(4):663–671

Boettiger C, Batt R (2020) Bifurcation or state tipping: assessing transition type in a model trophic cascade. J Math Biol 80(1):143–155

Carpenter SR, Cole JJ, Pace ML, Batt R, Brock WA, Cline T, Coloso J, Hodgson JR, Kitchell JF, Seekell DA et al (2011) Early warnings of regime shifts: a whole-ecosystem experiment. Science 332(6033):1079–1082

Chou T, D'Orsogna MR (2014) First passage problems in biology. In: First-passage phenomena and their applications, World Scientific, 306–345

Dakos V, Matthews B, Hendry AP, Levine J, Loeuille N, Norberg J, Nosil P, Scheffer M, De Meester L (2019) Ecosystem tipping points in an evolving world. Nat Ecol Evolut 3(3):355–362

Drury KL (2007) Shot noise perturbations and mean first passage times between stable states. Theor Popul Biol 72(1):153–166

Floris C (2019) First-passage time study of a stochastic growth model. Nonlinear Dyn 98(2):861–872

Francis TB, Abbott KC, Cuddington K, Gellner G, Hastings A, Lai Y-C, Morozov A, Petrovskii S, Zeeman ML (2021) Management implications of long transients in ecological systems. Nat Ecol Evolut 5(3):285–294

Gardiner CW et al (1985) Handbook of stochastic methods for physics, chemistry and the natural sciences, vol 3. Springer, Berlin

Grebenkov DS, Holcman D, Metzler R (2020) New trends in first-passage methods and applications in the life sciences and engineering. J Phys A: Math Theor 53(19):190301

Hastings A (2001) Transient dynamics and persistence of ecological systems. Ecol Lett 4(3):215–220

Hastings A, Abbott KC, Cuddington K, Francis T, Gellner G, Lai Y-C, Morozov A, Petrovskii S, Scranton K, Zeeman ML (2018) Transient phenomena in ecology. Science 361(6406):eaat6412

Hastings A, Abbott KC, Cuddington K, Francis TB, Lai Y-C, Morozov A, Petrovskii S, Zeeman ML (2021) Effects of stochasticity on the length and behaviour of ecological transients. J R Soc Interface 18(180):20210257

Jäger CG, Diehl S, Matauschek C, Klausmeier CA, Stibor H (2008) Transient dynamics of pelagic producer-grazer systems in a gradient of nutrients and mixing depths. Ecology 89(5):1272–1286

Kramers HA (1940) Brownian motion in a field of force and the diffusion model of chemical reactions. Physica 7(4):284–304
Kurella V, Tzou JC, Coombs D, Ward MJ (2015) Asymptotic analysis of first passage time problems inspired by ecology. Bull Math Biol 77(1):83–125
Liu A, Magpantay F (2022) A quantification of long transient dynamics. SIAM J Appl Math 82(2):381–407
Liu A, Magpantay FMG, Abdella K (2023) A framework for long-lasting, slowly varying transient dynamics. Math Biosci Eng 20(7):12130–12153
Ludwig D, Jones DD, Holling CS et al (1978) Qualitative analysis of insect outbreak systems: the spruce budworm and forest. J Anim Ecol 47(1):315–332
May RM (1977) Thresholds and breakpoints in ecosystems with a multiplicity of stable states. Nature 269(5628):471
McKenzie HW, Lewis MA, Merrill EH (2009) First passage time analysis of animal movement and insights into the functional response. Bull Math Biol 71:107–129
Morozov A, Abbott K, Cuddington K, Francis T, Gellner G, Hastings A, Lai Y-C, Petrovskii S, Scranton K, Zeeman ML (2020) Long transients in ecology: Theory and applications. Phys Life Rev 32:1–40
Nolting BC, Abbott KC (2016) Balls, cups, and quasi-potentials: quantifying stability in stochastic systems. Ecology 97(4):850–864
R Core Team (2023) R: a language and environment for statistical computing. R foundation for statistical computing, Vienna, Austria
Reimer J, Arroyo-Esquivel J, Jiang J, Scharf H, Wolkovich E, Zhu K, Boettiger C (2021) Noise can create or erase long transient dynamics. Thyroid Res 14(4):685–695
Scheffer M, Bascompte J, Brock WA, Brovkin V, Carpenter SR, Dakos V, Held H, Van Nes EH, Rietkerk M, Sugihara G (2009) Early-warning signals for critical transitions. Nature 461(7260):53
Strogatz SH (1994) Nonlinear dynamics and chaos: with applications to physics, biology, chemistry, and engineering. Cambridge, Westview
The MathWorks Inc (2020) Matlab version: 9.9.0 (r2020b)
Van Geest G, Coops H, Scheffer M, Van Nes E (2007) Long transients near the ghost of a stable state in eutrophic shallow lakes with fluctuating water levels. Ecosystems 10(1):37–47
Vortkamp I, Schreiber SJ, Hastings A, Hilker FM (2020) Multiple attractors and long transients in spatially structured populations with an Allee effect. Bull Math Biol 82:1–21
Zhang H, Xu W, Lei Y, Qiao Y (2019) Noise-induced vegetation transitions in the grazing ecosystem. Appl Math Model 76:225–237